Kinetic models for traffic flow resulting in a reduced space of microscopic velocities

Gabriella Puppo*[1], Matteo Semplice†[2], Andrea Tosin‡[3] and Giuseppe Visconti§[1]

[1]Università dell'Insubria, Como, Italy
[2]Università degli Studi di Torino, Torino, Italy
[3]Istituto per le Applicazioni del Calcolo "M. Picone", CNR, Roma, Italy

Abstract

We introduce a kinetic model for traffic flow, based on Boltzmann like binary interactions. We illustrate two possible examples of this type, using two different patterns to model interactions resulting in acceleration, both based on a parameter that describes the maximum acceleration of a vehicle. Under suitable and reasonable hypotheses on the microscopic interactions among vehicles, we can compute the asymptotic behaviour of the resulting kinetic distribution functions. In both cases, we find that these models permit to recover the phase change observed in experimental fundamental diagrams. Further, the analysis of the exact equilibria shows that it is possible to have the full richness of a kinetic approach with the simplicity of a space of microscopic velocities characterized by a small number of modes.

Keywords kinetic models, traffic flow, equilibrium distributions, discrete velocity models

MSC 76P05, 65Z05, 90B20

1 Introduction

In this work we discuss a kinetic traffic model characterized by the fact that drivers react to the presence of other vehicles, deciding whether to modify their speed according to the overall traffic conditions and to the particular velocity of the cars around them. Thus, the decision of whether to modify one's speed is modelled with a probability distribution, which depends on the local traffic density, or better, on the free space available, as we argue in [21]. The possible speeds available to the driver are naturally the driver's current speed, and a set of possible speeds which depend on the velocity of the vehicles ahead.

This framework permits to take the stochasticity of the drivers' behaviour into account, thanks to the probability distribution which assigns a weight to the possible driver's decisions, while maintaining the general kinetic setting, based on binary interactions. In this sense, the model proposed here generalizes a previous kinetic model for traffic flow, introduced in [6, 7].

*gabriella.puppo@uninsubria.it
†matteo.semplice@unito.it
‡a.tosin@iac.cnr.it
§giuseppe.visconti@uninsubria.it

However, here we introduce a few important generalizations. The model [6] considers a *discrete* lattice of velocities available, and the possible outcomes of an interaction depend on the particular lattice chosen. Here the effort is to introduce a few parameters, namely, the maximum speed $V_{\max}$ of cars, and the velocity jump Δv which are based on the actual characteristics of the flow. For instance, $V_{\max}$ can be dictated by the physical characteristics of vehicles, or on local speed limitations, while Δv is a parameter that depends on the mechanical characteristics of vehicles. In the section on macroscopic properties §5, we show that Δv is related to the maximum acceleration, and we discuss how this parameter can be chosen through experimental data used by Lebacque, [13]. Thus the model discussed here is based on a continuous and bounded velocity space, and on a parameter Δv which controls the maximum acceleration. Its solution is the distribution function describing the probability of finding a vehicle with a given speed, at a given time.

The purpose of kinetic theory for traffic flow is to provide an aggregate representation of the distribution of vehicles on the road, thanks to a detailed characterization of the microscopic interactions which play an important role in the macroscopic behaviour of the flow. Several kinetic approaches have been proposed, starting from the pioneering work of [19, 20] and later [17]. For more recent reviews on kinetic traffic models, see [12]. The goal is to obtain information on the macroscopic carateristics of the flow, without assuming previous knowledge on the dependence of the mean velocity on the local density of traffic, as is done in standard macroscopic traffic models. See in particular the prototype of macroscopic models, [15], or the reviews in [22, 18]. More refined macroscopic models consider a system of equations, instead of a single equation, see [2], and/or they prescribe different flow conditions at certain stages, building phase transitions within the flow, [16, 14], but still it is necessary to complete the model with a closure law, derived from heuristic or physical arguments, or from experimental data. Kinetic models provide quite naturally a closure law, which is linked in general to the equilibria of the kinetic model. Several models provide interesting ideas and tools, see [11, 10], where the drivers react to non local interactions, or [8, 9], where the interaction is modelled with a Vlasov type relaxation towards a desired speed. Another approach to derive closure laws can be obtained through microscopic "follow the leader" models [23], see [1]. For a review on the derivation of macroscopic traffic models from the microscopic "follow the leader" approach and from the mesoscopic kinetic approach, see [3].

In this work, we follow the classical Boltzmann like setting of binary interactions. The cross section of Boltzmann models which gives the probability of an interaction, is replaced here with a probability distribution which depends on the local mean traffic conditions. Further, we suppose that a vehicle driving at speed v_*, meeting a *slower* vehicle with speed v^*, can either brake to the speed v^*, or keep its previous velocity, thus overtaking the slower vehicle. Acceleration can occur when a driver meets a *faster* vehicle. In this case, its new velocity is chosen within $v_*, v_* + \Delta v$, where Δv is the maximum speed change available in a unit time.

We propose two models that follow the framework just described, one based on a quantized velocity jump, i.e. if acceleration occurs, the new speed is $v_* + \Delta v$, (δ model), the other one is based on a continuous uniform distribution between v_* and $v_* + \Delta v$ (χ model), see also [11].

The δ and the χ models are discussed in depth in §3 and 4. There we compute the exact equilibrium distributions of the δ model, proving that at equilibrium the possible velocities are quantized, according to the parameter Δv. This in turn permits to write explicitly the exact equilibrium distribution of the δ model, showing that the equilibrium solution (and therefore the macroscopic characteristics of the flow) depend on a few velocity values, namely the integer multiples of the velocity jump Δv. In §4, we show the somewhat surprising result that the equilibrium distributions of the χ model yield a macroscopic flow that is extremely well approximated by the closure law resulting from the δ model. This is illustrated in the final section §5, where

the fundamental diagrams, that is the flux-density diagrams, obtained by the two models tend to coincide, under grid refinement. Further, we compute the macroscopic acceleration induced by the model, proving in particular the link between Δv and the acceleration.

We end the paper with a section summarising the main results of this work, and proposing possible applications and further developments. Finally, the details of the matrix elements resulting from the discretization of the χ model are written in an Appendix.

2 The general form of the kinetic model

In this section, we present a kinetic traffic model which is a generalization of [6]. Unlike [6], the present model is defined on a continuous velocity space, and it is characterized by a parameter Δv related to the typical acceleration of a vehicle. We start from a general construction, and then we derive two simplified models. Next, we show that the simplified models permit to describe the complexity of the equilibrium solutions with a very small number of discrete velocities.

We will focus only on the space homogeneous case, because we want to investigate the structure of the collision term, and of the resulting equilibrium distributions.

Let $f = f(t, x, v)$ be the *kinetic distribution function* such that $f(t, x, v)dxdv$ gives the number of vehicles at place $[x, x + dx]$ with velocity in $[v, v + dv]$ at time t. Space homogeneity can be translated mathematically by assuming that the function f does not depend on the space variable x. Therefore, the statistical distribution of vehicles is given by the function:

$$f = f(t, v) : \mathbb{R}^+ \times [0, V_{\max}] \to \mathbb{R}^+,$$

where $V = [0, V_{\max}]$ is the domain of the microscopic speeds and $V_{\max}$ is the maximum speed, which may depend on the mechanical characteristics of the vehicles, on imposed speed limits, environmental conditions (such as quality of the road, weather conditions, etc).

As usual, macroscopic quantities are obtained as moments of the distribution function f with respect to the velocity v:

$$\rho(t) = \int_V f(t, v)dv, \quad (\rho u)(t) = \int_V v f(t, v)dv$$

where ρ is the *density*, i.e. the number of vehicles per unit length (tipically, kilometers), u is the *macroscopic speed* and ρu is the *flux* of vehicles. Note that ρ can also be interpreted as the reciprocal of the average distance between cars, see [2].

Here we consider a Boltzmann-type kinetic model for vehicular traffic, in which the relaxation to equilibrium is due to binary interactions. In the homogeneous case, the model can be written as

$$\partial_t f(t, v) = Q[f, f](t, v) \tag{1}$$

where $J[f, f](t, v)$ is the *collisional operator* and it describes the change of f in time given by the microscopic interactions among vehicles. For mass conservation to hold, the collision term must satisfy

$$\int_V Q[f, f](t, v)dv = 0.$$

In fact, this ensures that, in the space homogeneous case, the density remains constant during the evolution of the flow:

$$\frac{d}{dt}\rho(t) = \partial_t \int_V f(t, v)dv = 0.$$

We split the collisional operator into a gain term $G[f,f]$ and a loss term $L[f,f]$ that model statistically the interactions which lead to acquire or to loose the test speed v.

Denoting with $A(v_*\to v|v^*)$ the probability that the velocity $v \in V$ will result from a microscopic interaction between candidate vehicles with velocity v_* and field vehicles with speed v^*, the model writes as an integro-differential equation

$$\partial_t f(t,v) = \underbrace{\int_V \int_V \eta(v_*,v^*) A(v_*\to v|v^*) f(t,v_*) f(t,v^*) dv_* dv^*}_{G[f,f]} - \underbrace{f(t,v) \int_V \eta(v,v^*) f(t,v^*) dv^*}_{L[f,f]} \quad (2)$$

in which $\eta(v_*,v^*)$ is the *interaction rate* which may depend on the relative speed of the interacting vehicles, e.g. $\eta(v_*,v^*) = |v_* - v^*|$ as in [10, 4]. This choice would make the model richer, however, in [21], we found that a constant interaction rate is already sufficient to account for many aspects of the complexity of traffic. Another possibility is to consider η as dependent on the local congestion of the road, that is $\eta = \eta(\rho)$. However this is not relevant in the homogeneous case, where ρ is constant, and therefore η affects only the relaxation time towards equilibrium. Thus in this paper we will set $\eta(v_*,v^*;\rho) = \eta$.

Notation. In the whole paper, in order to shorten formulas, we adopt the following traditional shorthand $f(t,v_*) = f_*$, $f(t,v^*) = f^*$, etc. Note that f^* and f_* are not different distribution functions, but the evaluation of the same $f(t,v)$ at two different points v_* and v^*.

We will suppose that A depends also on the macroscopic density ρ in order to account for the influence of the macroscopic traffic conditions (local road congestion) on the microscopic interactions among vehicles, see [20, 10, 9, 21]. Thus, we suppose that A fulfills

Assumption 1.

$$A(v_*\to v|v^*;\rho) \geq 0, \quad \text{and} \int_V A(v_*\to v|v^*;\rho) dv = 1, \quad \text{for } v_*, v^*, v \in V,\ \rho \in [0,\rho_{\max}]$$

where $\rho_{\max}$ is the maximum density of vehicles and it can be chosen as the maximum number of vehicles per unit length in bumper-to-bumper conditions.

Remark 1. Any transition probability density A that satisfies Assumption 1 guarantees mass conservation since

$$\partial_t \int_V f(t,v) dv = \int_V [G(v) - L(v)] dv = \int_V \int_V f(t,v_*) f(t,v^*) dv_* dv^* - \int_V f(t,v) dv \int_V f(t,v^*) dv^* = \rho^2 - \rho^2 = 0$$

It is convenient to split $V \times V$ into

$$\Omega_1 = \left\{(v_*,v^*) \in [0,V_{\max}]^2 : v_* \leq v^*\right\} \quad (3)$$
$$\Omega_2 = \left\{(v_*,v^*) \in [0,V_{\max}]^2 : v_* > v^*\right\},$$

and consequently the gain term $G[f,f](t,v)$ as

$$G[f,f](t,v) = \underbrace{\int_{\Omega_1} \eta A_1(v_*\to v|v^*;\rho) f(t,v_*) f(t,v^*) dv_* dv^*}_{G_1[f,f](t,v)} + \underbrace{\int_{\Omega_2} \eta A_2(v_*\to v|v^*;\rho) f(t,v_*) f(t,v^*) dv_* dv^*}_{G_2[f,f](t,v)}. \quad (4)$$

Here A_1 and A_2 are the projections of the transition probability density A onto the sets Ω_1 and Ω_2 respectively. Note that the modelling of acceleration will be contained in A_1, because a candidate vehicle travelling at speed v_* may decide to accelerate when it meets a faster vehicle, provided that there is free space ahead. The modelling of overtaking and braking will be contained in A_2, because in this case the candidate vehicle at speed v_* is interacting with a field vehicle travelling at a slower speed v^*.

2.1 Choice of the probability density A

The probability density A assignes a post-interaction speed in a non-deterministic way, consistently with the intrinsic stochasticity of the drivers' behaviour. The construction of A is at the core of the model we propose. It is obtained with a very small set of rules.

- if $(v_*, v^*) \in \Omega_1$, i.e. the candidate vehicle is slower than the field vehicle, the post-interaction rules are:

  Do nothing: the candidate vehicle keeps its pre-interaction speed with probability $1-P_1$, thus $v = v_*$;

  Accelerate: the candidate vehicle accelerates to a velocity $v > v_*$ with probability P_1;

- if $(v_*, v^*) \in \Omega_2$, i.e. the candidate vehicle is faster than the field vehicle, the post-interaction rules are:

  Do nothing: the candidate vehicle keeps its pre-interaction velocity with probability P_2, so $v = v_*$, thus overtaking the field vehicle;

  Brake: the candidate vehicle decelerates to the velocity $v = v^*$ with probability $1 - P_2$, thus following the leading vehicle;

From the previous rules, we observe that both probability densities A_1 and A_2 have a term that will be proportional to a Dirac delta function at $v = v_*$, due to interactions in which the pre-interaction microscopic speed is preserved (the two "Do nothing" alternatives). Note that these are "false gains" for the distribution f, because the number of vehicles with speed v is not altered by these interactions.

In [10] Klar and Wegener assume that the velocity after acceleration is uniformly distributed over a range of speeds between v_* and $v_* + \alpha(V_{\max} - v_*)$, where α is supposed to depend on the local density; in a similar way, the output velocity from a braking interaction is assumed to be uniformly distributed in $[\beta v^*, v^*]$, with $\beta \in [0, 1]$.

Instead, the rules above assign the speed after braking as proposed in [19] and used also in [6, 7] in the context of a discrete velocity model. Namely, we suppose that if a vehicle brakes, interacting with a slower vehicle, it will slow down to the speed v^* of the leading vehicle, thus, after the interaction, $v = v^*$, and the field vehicle will remain behind the leading vehicle. For the post-interaction speed due to acceleration we propose two different models.

Quantized acceleration (δ model): we will suppose that the output velocity v is obtained by accelerating instantaneously from v_* to the velocity $\min\{v_* + \Delta v, V_{\max}\}$. Considering all possible outcomes, the resulting probability distribution is

$$A(v_* \to v | v^*; \rho) = \begin{cases} (1-P_1)\delta_{v_*}(v) + P_1 \delta_{\min\{v_*+\Delta v, V_{\max}\}}(v), & \text{if } (v_*, v^*) \in \Omega_1 \\ (1-P_2)\delta_{v^*}(v) + P_2 \delta_{v_*}(v), & \text{if } (v_*, v^*) \in \Omega_2. \end{cases} \tag{5}$$

Uniformly distributed acceleration (χ model): here we assume that the new velocity v is uniformly distributed between v_* and $\min\{v_* + \Delta v, V_{\max}\}$. The resulting probability distribution is

$$A(v_* \to v|v^*;\rho) = \begin{cases} (1-P_1)\delta_{v_*}(v) + P_1 \frac{\chi_{[v_*,\min\{v_*+\Delta v,V_{\max}\}]}(v)}{\min\{v_*+\Delta v,V_{\max}\}-v_*}, & \text{if } (v_*,v^*) \in \Omega_1 \\ (1-P_2)\delta_{v^*}(v) + P_2\delta_{v_*}(v), & \text{if } (v_*,v^*) \in \Omega_2. \end{cases} \tag{6}$$

Note that the δ model (5) of A may seem as a continuous extension of the model [6, 7] which was based on a discrete velocity space. However, in [6, 7] the *acceleration parameter* Δv is chosen as the distance between two adjacent discrete velocities, thus Δv depends on the number of elements in the speed lattice. In this work, Δv is a physical parameter that represents the ability of a vehicle to change its pre-interaction speed v_*. With this choice, Δv will not depend on the discretization of the velocity space and the maximum acceleration is bounded, as in [13]. In contrast, deceleration can be larger than Δv, and this fact reflects the hypothesis that drivers tend to brake immediately if the traffic becomes more congested, while they react more slowly when they can accelerate (see the concept of *traffic hysteresis* in [23] and references therein).

In the following, the probabilities P_1 and P_2 are taken as $P = P_1 = P_2$ and P will be a function of the local density only, as assumed for instance in [20] where $P = 1 - \rho/\rho_{\max}$. More generally P should be a decreasing function of ρ, see also [8] or [22]. For instance in [21] we have taken

$$P = 1 - \left(\frac{\rho}{\rho_{\max}}\right)^{\gamma}, \tag{7}$$

where $\gamma \in (0,1)$ can be chosen to better fit experimental data. In [6] $P = \alpha(1 - \rho/\rho_{\max})$, with $\alpha \in [0,1]$ as a parameter describing environmental conditions, for instance road or weather conditions. In more sophisticated models, one could also choose P as a function of the relative velocities of interacting vehicles, but we will not explore this possibility in the present work.

Remark 2. Both choices (5) and (6) for A include terms of the form $\delta_{v_*}(v)$ which actually describe false gains mentioned above, because the velocity of the candidate vehicle does not change. They are automatically compensated by false losses, because the classical kinetic loss term of equation (2) can be rewritten as

$$L[f,f](t,v) = \int_V \int_V \eta \delta_{v_*}(v) f_* f^* dv^* dv_*$$

and already accounts for them.

3 The δ velocity model

Using the expression (5) for A, we rewrite the gain term in (2) as:

$$\begin{aligned} G[f,f] =& \eta \int_{\Omega_1} \left[(1-P)\delta_{v_*}(v) + P\delta_{\min\{v_*+\Delta v,V_{\max}\}}(v)\right] f_* f^* dv_* dv^* \\ &+ \eta \int_{\Omega_2} \left[(1-P)\delta_{v^*}(v) + P\delta_{v_*}(v)\right] f_* f^* dv_* dv^* \end{aligned}$$

where Ω_1, Ω_2 are defined in (3).

We compute explicitly the restrictions G_1 and G_2 of the gain term on the sets Ω_1 and Ω_2. In G_1 the Dirac delta function at $v = \min\{v_* + \Delta v, V_{\max}\}$ can be split as

$$\delta_{\min\{v_*+\Delta v,V_{\max}\}}(v) = \begin{cases} \delta_{v_*+\Delta v}(v), & \text{if } v_* \in [0, V_{\max} - \Delta v] \\ \delta_{V_{\max}}(v), & \text{if } v_* \in [V_{\max} - \Delta v, V_{\max}] \end{cases}$$

because the velocity jump of size Δv, leading to the output velocity $v = v_* + \Delta v$, can be performed only if $v_* \leq V_{\max} - \Delta v$. If instead $v_* \in [V_{\max} - \Delta v, V_{\max}]$, the post-interaction velocity will be $v = V_{\max}$. Thus G_1 can be written as:

$$\begin{aligned} G_1[f,f](t,v) =& \eta(1-P)f(t,v)\int_v^{V_{\max}} f^* dv^* \\ &+ \eta P f(t, v-\Delta v) H_{\Delta v}(v) \int_{v-\Delta v}^{V_{\max}} f^* dv^* \\ &+ \eta P \delta_{V_{\max}}(v) \int_{V_{\max}-\Delta v}^{V_{\max}} f_* dv_* \int_{v_*}^{V_{\max}} f^* dv^*. \end{aligned}$$

where $H_\alpha(x)$ denotes the Heaviside step function with jump located in α. The last term in the expression for G_1 means that, as a result of the microscopic interactions, the mass $P\int_{V_{\max}-\Delta v}^{V_{\max}} f_* dv_* \int_{v_*}^{V_{\max}} f^* dv^*$ is assigned entirely to $f(t, V_{\max})$.

The projection of the gain operator G over Ω_2 is

$$G_2[f,f](v) = \eta(1-P)\int_V \delta_{v^*}(v) f^* dv^* \int_{v^*}^{V_{\max}} f_* dv_* + \eta P \int_V \delta_{v_*}(v) f_* dv_* \int_0^{v_*} f^* dv^*$$

which can be rewritten as

$$G_2[f,f](v) = \eta(1-P)f(t,v)\int_v^{V_{\max}} f_* dv_* + \eta P f(t,v)\int_0^v f^* dv^*.$$

Globally, the gain term of the δ model is written as

$$\begin{aligned} G[f,f] =& \eta(1-P)f(t,v)\left[\int_v^{V_{\max}} f^* dv^* + \int_v^{V_{\max}} f_* dv_*\right] + \eta P f(t,v)\int_0^v f^* dv^* \\ &+ \eta \begin{cases} P f(t, v-\Delta v) H_{\Delta v}(v) \int_{v-\Delta v}^{V_{\max}} f^* dv^* & \text{if} \quad v \in [0, V_{\max} - \Delta v) \\ P\delta_{V_{\max}}(v) \int_{V_{\max}-\Delta v}^{V_{\max}} f_* dv_* \int_{v_*}^{V_{\max}} f^* dv^* & \text{if} \quad v \in [V_{\max} - \Delta v, V_{\max}] \end{cases} \end{aligned} \tag{8}$$

Note that, in non space-homogeneous models, f_* and f^* may refer to distributions evaluated at different locations in space, see for instance [10] and [11]. For this reason we write the gain term with the two integrals over field and candidate particles separately.

3.1 Discretization of the model

In order to study the properties of the model, we consider a discretization of the velocity space. We suppose that the acceleration parameter Δv is a fixed parameter of the model. For simplicity, we suppose that $\Delta v = V_{\max}/T$ with $T \in \mathbb{N}$. The study becomes simpler if we choose the discretization parameter δv such that $\Delta v = r\delta v$, so that Δv corresponds to an integer number of intervals in the velocity discretization. Thus we will take $T \in \mathbb{N}$ fixed, while $r = \frac{N-1}{T}$ will depend on the number of grid points N.

We define the velocity cells $I_j = [(j - \frac{3}{2})\delta v, (j - \frac{1}{2})\delta v] \cap [0, V_{\max}]$, for $j = 1, \ldots, N$. Note that all cells have amplitude δv except I_1 and I_N which have amplitude $\delta v/2$. The velocity grid nodes, located at the center of each cell, are $v_1 = \delta v/4, v_N = V_{\max} - \delta v/4$, and $v_j = (j-1)\delta v$ for $j = 2, \ldots, N-1$. This choice is convenient for computations, see §5, because all grids with $r > 1$ contain all the points of the coarser mesh with $r = 1$ (except the first and the last point).

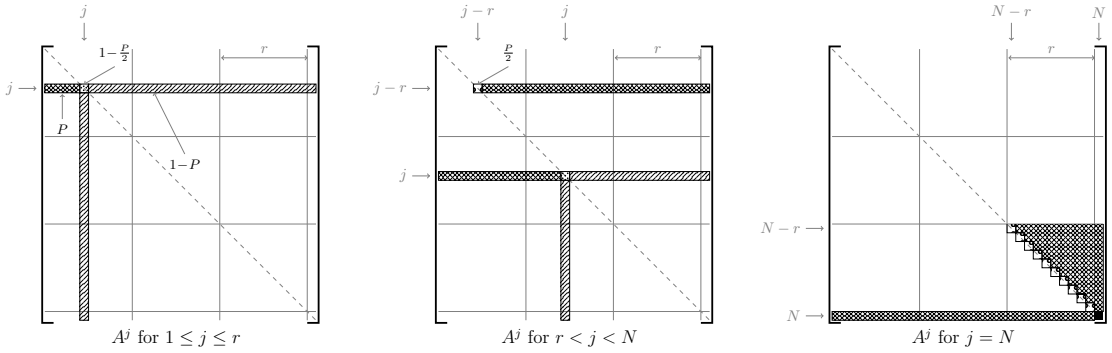

Figure 1: Structure of the probability matrices of the δ model.

In order to discretize the model, we approximate the velocity distribution with the piece-wise constant function

$$f(t,v) = \sum_{j=1}^{N} f_j(t) \frac{\chi_{I_j}(v)}{|I_j|} \tag{9}$$

where f_j represents the number of vehicles travelling with velocity $v \in I_j$.

By integrating the kinetic equation (1) over the cells I_j we obtain the following system of ordinary differential equations

$$f_j'(t) = Q_j[f,f](t) = \int_{I_j} Q[f,f](t,v)dv \tag{10}$$

whose initial condition $f_1(0), \ldots, f_N(0)$ are such that:

$$\sum_{j=1}^{N} f_j(0) = \int_V f(t=0,v)dv = \rho_0$$

and ρ is the initial density, which remains constant in the spatially homogeneous case.

By computing the right hand side of the ODE system, we obtain

$$\frac{1}{\eta}Q_j[f,f](t) = (1-\frac{P}{2})f^j f_j + Pf_j\sum_{k=1}^{j-1} f^k + (1-P)f_j\sum_{k=j+1}^{N} f^k \tag{11a}$$
$$+ (1-P)f^j\sum_{h=j+1}^{N} f_h - f_j\sum_{k=1}^{N} f^k, \qquad \text{for } j=1,\dots,r$$

$$\frac{1}{\eta}Q_j[f,f](t) = \underbrace{\frac{P}{2}f^{j-r}f_{j-r}} + (1-\frac{P}{2})f^j f_j + \underbrace{Pf_{j-r}\sum_{k=j-r+1}^{N} f^k} + Pf_j\sum_{k=1}^{j-1} f^k \tag{11b}$$
$$+ (1-P)f_j\sum_{k=j+1}^{N} f^k + (1-P)f^j\sum_{h=j+1}^{N} f_h - f_j\sum_{k=1}^{N} f^k, \quad \text{for } j=r+1,\dots,N-1$$

$$\frac{1}{\eta}Q_N[f,f](t) = \underbrace{\frac{P}{2}\sum_{h=N-r}^{N-1} f^h f_h} + f^N f_N + \underbrace{P\sum_{h=N-r}^{N-1}\sum_{k=h+1}^{N} f^k f_h} + Pf_N\sum_{k=1}^{N-1} f^k - f_N\sum_{k=1}^{N} f^k, \tag{11c}$$

In the formulae above, the distribution of the field and of the candidate vehicles are distinguished by the position of the index of the components of $\mathbf{f}$: bottom right for the candidate vehicles (as f_h), top right for the field vehicles (f^k). The terms with a wavy underline are those deriving from the acceleration term. The structure of the model is more readable in vector form:

$$\frac{d}{dt}f_j = \eta\left[\mathbf{f}^\mathsf{T}A_\delta^j\mathbf{f} - \mathbf{f}^\mathsf{T}\mathbf{e}_j\mathbf{1}_N^\mathsf{T}\mathbf{f}\right], \quad j=1,\dots,N \tag{12}$$

where $\mathbf{f}=[f_1,\dots,f_N]^\mathsf{T}\in\mathbb{R}^N$, $\mathbf{e}_j\in\mathbb{R}^N$ denotes the vector with a 1 in the j-th component and 0's elsewhere, $\mathbf{1}_N^\mathsf{T}=[1,\dots,1]\in\mathbb{R}^N$. The matrices A_δ^j have a sparse structure, which is shown in Fig. 1.

As it can be checked using (11), these matrices are stochastic with respect to the index j, i.e. $\sum_{j=1}^N\left(A_\delta^j\right)_{hk}=1$, $\forall\, h,k\in\{1,\dots,N\}$. This property comes from Assumption 1, and it guarantees mass conservation.

In the figure, the nonzero elements are shaded with different hatchings, corresponding to the different values of the elements, as indicated in the first two panels.

Recall that the elements of the matrix A_{hk}^j are the probability that the candidate vehicle with velocity in I_h interacting with a field vehicle with velocity in I_k will acquire a velocity in I_j. The fact that these matrices are sparse means that a velocity in I_j can be acquired only for special values of the velocity of candidate and field vehicles. In particular, the j-th row of the matrix A^j contains the probability of what we called "false gains" in Remark 2, that is the probability that the candidate vehicle *does not* change its speed. The non zero elements of the j-th column contains the probability that a candidate vehicle acquires a speed in I_j by braking down to the speed of the leading vehicle. The non zero row, located at $h=j-r$, contains the probability that the candidate vehicle accelerates by Δv, acquiring therefore a velocity in $I_j=I_h+\Delta v$. The band between the rows $h=j-r$ and $h=j$ is filled with zeroes because the acceleration is quantized, in the δ model. This band will be filled by non zero elements in the χ model, where the acceleration is distributed uniformly between $[0,\Delta v]$.

The structure of the matrices A_{hk}^j determines the equilibrium of the system. In Figure 2 we show the function $f^\infty(v)=\lim_{t\to\infty}f(t,v)$ for a few typical cases. In all numerical tests we take

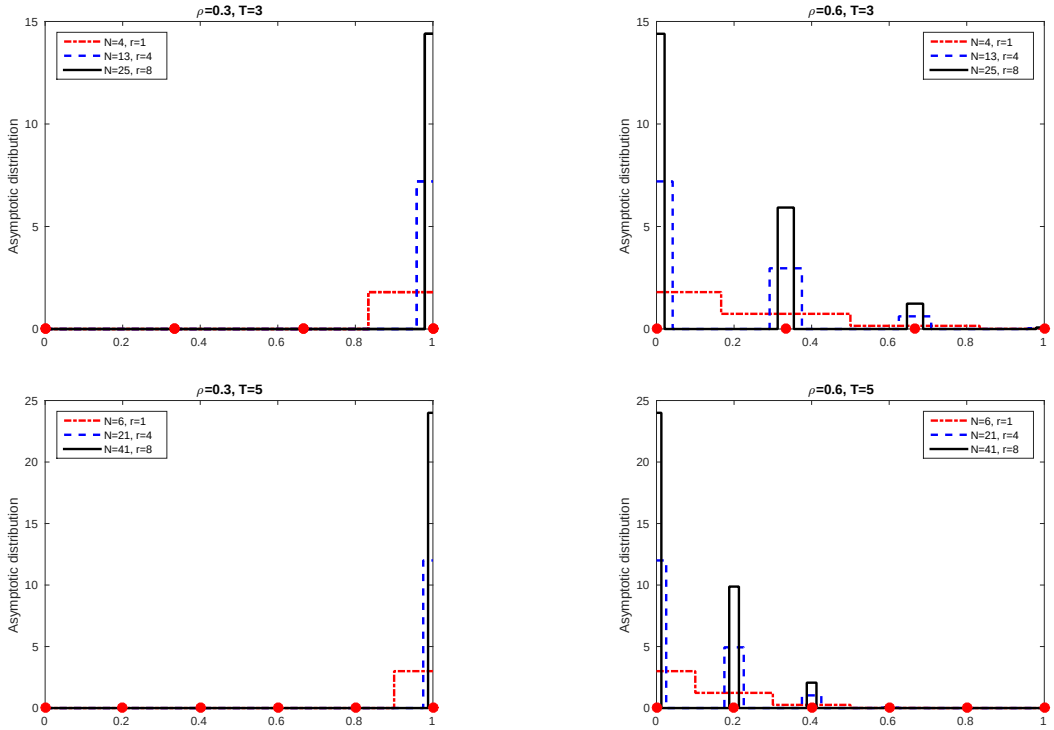

Figure 2: Approximation of the asymptotic kinetic distribution function obtained with two acceleration terms $\Delta v = 1/T$, $T = 3$ (top), $T = 5$ (bottom), and $N = rT + 1$ velocities, with $r \in \{1, 4, 8\}$; $\rho = 0.3$ (left) and $\rho = 0.6$ (right) are the initial densities. We mark with red circles on the x-axes the velocities (or grid points) of the discretized model with $N = T + 1$.

$P = 1 - \rho$, with $V_{\max} = \rho_{\max} = 1$. As initial macroscopic densities, we choose $\rho_0 = 0.3, 0.6$ (plots to the left and right of the figure). We consider two values for the acceleration parameter, $\Delta v = V_{\max}/T$, $T = 3, 5$ (top and bottom of the figure). The number of velocities in the grid is taken as $N = rT + 1$, with $r \in \{1, 4, 8\}$. The three curves in each plot contain the data for the cell averages of the equilibrium distribution for the different values of r. It is clear that in all cases, $f^\infty(\rho_0, v)$ approaches a series of delta functions, centered on the velocity grid points induced by the special velocity grid obtained with $r = 1$, which are indicated in the picture by red dots on the horizontal axis.

As time goes to infinity the number of non zero values of the steady-state distribution f^∞ is univocally determined by the acceleration term $\Delta v = V_{\max}/T$. More precisely, the kinetic function f^∞ is not identically zero only on the $T + 1$ cells, $V_1, V_r, V_{2r}, \ldots, V_N$.

Remark 3. Similar considerations hold if N is not a multiple of T. In this case we consider $r = \lfloor \frac{N-1}{T} + \frac{1}{2} \rfloor$, and we will find again that only the values of f on the velocity nodes corresponding to $v_k = \Delta v(k-1), k = 1, \ldots T + 1$ are non zero, as $\delta v \to 0$.

The evolution towards equilibrium of the distribution function is shown in Fig. 3. In this figure, $\Delta v = V_{\max}/3$, and the different plots show the evolution of f towards equilibrium, starting from a uniform initial distribution, namely $f_j(t = 0) = \rho/N, \forall j = 1, \ldots, N$, for $r = 1$ (green), $r = 2$ (blue) and $r = 3$ (red), which correspond to $N = 4, 7$ and 10 velocity grid points respectively.

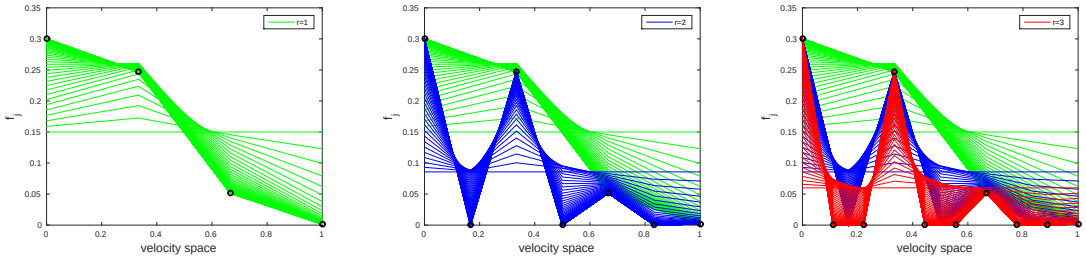

Figure 3: Evolution towards equilibrium of the discretized solution for model (12) with $N = 4$ (green), $N = 7$ (blue) and $N = 10$ (red) grid points. The acceleration parameter Δv is taken as $V_{\max}/3$. Black circles indicate the equilibrium values.

Note that a different dynamics towards equilibrium is observed, for different values of the number N of grid points, but as equilibrium is approached, the values of f go toward zero, except for the velocities v_j corresponding to integer multiples of Δv.

To study the structure of the solutions of system (12), we first recall a result from [5], where the existence and well posedness of the solution of such systems is proven.

Theorem 4. (Delitala-Tosin) Let $f_0(v) \geq 0$, with $\rho = \int f_0(v)\, dv$, be the initial condition for the system

$$\frac{d}{dt} f_j = \mathbf{f}^T A^j \mathbf{f} - \mathbf{f}^T \mathbf{e}_j \mathbf{1}_N^T \mathbf{f}, \quad j = 1, \ldots, N,$$

where the matrices A^j are stochastic matrices with respect to the index j, i.e. $\sum_j A^j_{hk} = 1$ for all h, k. Then there exists $t_* > 0$ such that the system admits a unique non-negative local solution $f \geq 0$ satisfying the a priori estimate

$$||f(t)||_1 = ||f_0||_1 = \rho \qquad \forall t \in (0, t_*].$$

The following theorem proves the structure of the equilibria that we have already observed in the numerical results.

Theorem 5. For any fixed $\Delta v = V_{\max}/T$, $T \in \mathbb{N}$, let $\mathbf{f}_r(\rho)$ denote the equilibrium distribution function of the ODE's system (10), obtained on the grid with spacing δv given by $\Delta v = r\delta v$ with $r = (N-1)/T \in \mathbb{N}$. Then

$$(\mathbf{f}_r)_j = \begin{cases} (\mathbf{f}_1)_{(j-1)/T} & \mathrm{mod}(j-1, T) = 0 \\ 0 & \text{otherwise} \end{cases} \tag{13}$$

is the unique stable equilibrium distribution, and the values of $\mathbf{f}_1$ depend uniquely on the initial density ρ, with $\sum_{k=1}^{T+1} (\mathbf{f}_1)_k = \rho$.

Proof. We already know from Theorem 4 that the solution of (10) exists is non-negative and is uniquely determined by the initial condition.

To prove the statement, we compute explicitly the equilibrium solutions of (10), using the explicit expression of the collision kernel given in (11a), (11b) and (11c). Since here we are interested in the solutions of the homogeneous problem, we will take identical distributions for the candidate and the field vehicles, i.e. $f_j \equiv f^j$.

For $j = 1$, using the expression (11a), adding the loss term, and using the fact that $\sum_k f_k = \rho$ we obtain

$$\frac{d}{dt} f_1 = 0 \quad \Leftrightarrow \quad \left(\frac{3P-2}{2}\right) f_1^2 + (1-2P)\, \rho f_1 = 0. \tag{14}$$

This is a quadratic equation for f_1, which has the two roots $f_1 = 0$ and $f_1 = \rho(2P-1)/(\frac{3}{2}P-1)$. It is easy to see that one solution is stable, and the other one unstable, depending on the value of P. Here we are interested only in the stable root, so we find

$$(\mathbf{f}_r)_1 = \begin{cases} 0 & P \geq \frac{1}{2} \\ 2\frac{2P-1}{3P-2}\rho & \text{otherwise} \end{cases} \tag{15}$$

Thus, no vehicle is in the lowest speed class I_1 if $P \leq \frac{1}{2}$, which, for the simple case $P = 1 - \rho$ means that all cars are moving if $\rho \leq \frac{1}{2}$.

The $j = 1$ case we just computed is typical. Also for larger values of j, we find a quadratic equation for the unknown f_j, which involves only previously computed values of $f_k, k < j$. Thus, we can easily compute successively all components of $\mathbf{f}_r$.

For $2 \leq j \leq r$, the equilibrium equation is

$$\left(\frac{3P-2}{2}\right) f_j^2 + \left[(3P-2)\sum_{k=1}^{j-1} f_k + (1-2P)\,\rho\right] f_j = 0.$$

Start from $j = 2$. Clearly, for $P > \frac{1}{2}$, substituting eq. (15), we again have $(\mathbf{f}_r)_2 = 0$. For $P < \frac{1}{2}$, the equation for f_2, with f_1 given by (15), becomes

$$\left(\frac{3P-2}{2}\right) f_2^2 - (1-2P)\,\rho f_2 = 0.$$

Comparing with the equation for f_1, we see that now the stable root is $f_2 = 0$. Thus, at equilibrium, we have $(\mathbf{f}_r)_2 \equiv 0$, for all values of P. Analogously, it is easy to see that $(\mathbf{f}_r)_j \equiv 0, \forall j = 2, \dots r$.

For $j \geq r + 1$, in place of (11a), we use (11b), which contains two extra terms:

$$\frac{P}{2} f_{j-r}^2 + (1-P) f_{j-r} \sum_{k=j-r+1}^{N} f_k.$$

If we consider $r + 1 < j < 2r + 1$, then $f_{j-r} = 0$ from the previous step, and the equation is identical to a case we have already seen, so $(\mathbf{f}_r)_j = 0$ for $r + 1 < j < 2r + 1$. If instead $j = r + 1$, then $f_{j-r} = f_1$. The new terms are certainly zero for $P \geq \frac{1}{2}$. So again we find $(\mathbf{f}_r)_{r+1} = 0$ for $P \geq \frac{1}{2}$, because the equation becomes identical to what we have already seen. If $P < \frac{1}{2}$, substituting the expression for f_1, the equation for f_{r+1} becomes

$$\left(\frac{3P-2}{2}\right) f_{r+1}^2 + (2P-1)\rho f_{r+1} + \frac{2P(2P-1)}{3P-2}\rho^2 = 0.$$

This equation has a negative and a positive real root, which is stable. Thus

$$(\mathbf{f}_r)_{r+1} = \begin{cases} 0 & P \geq \frac{1}{2} \\ \rho\frac{1-2P+\sqrt{1-4P^2}}{3P-2} & \text{otherwise.} \end{cases} \tag{16}$$

Clearly, this procedure can be repeated. For $(l-1)r < j < lr + 1$, the equation for f_j is

$$\frac{df_j}{dt} = \frac{3P-2}{2} f_j^2 + (1-2P)\rho f_j + (3P-2) f_j \sum_{h=0}^{l-1} f_{rh+1}$$

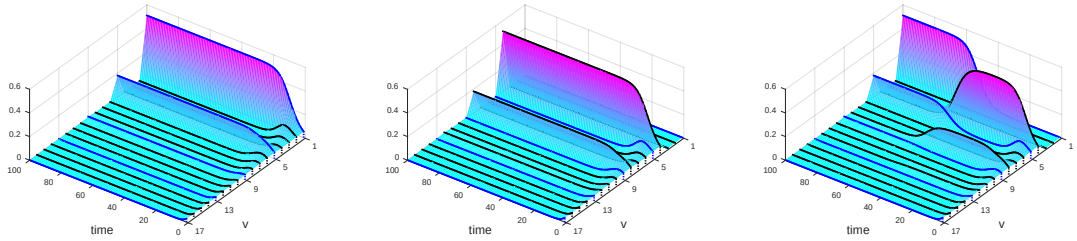

Figure 4: Evolution towards equilibrium, $\rho = 0.7$, $T = 4$, $N = 17$. Left: $f_j(t = 0) \equiv \rho/N$. Middle: $f_j(t = 0) = 0, j = 1, 2, 3$, $f_j(t = 0) \equiv (\rho/(N - 3)), j > 3$. Right: $f_1 = \epsilon = 10^{-6}, f_2 = f_3 = 0$ and $f_j(t = 0) \equiv ((\rho - \epsilon)/(N - 3))$. The thick lines highlight the components f_j and the blue ones are for those that appear in stable equilibria, i.e. with $j = kr + 1$ for $k = 0, \dots, T$.

which clearly gives $f_j = 0$ for $P \geq \frac{1}{2}$. For $P < \frac{1}{2}$, again the largest root is positive. One root is $f_j = 0$, the other one is

$$f_j = \frac{2}{3P - 2} \left((2P - 1)\rho + (2 - 3P) \sum_{h=0}^{l-1} f_{rh+1} \right),$$

where the numerator is clearly positive. Thus again the largest root is $f_j = 0$. From these considerations, the thesis easily follows. Just note that for the last value, f_N, we use mass conservation

$$(\mathbf{f}_r)_{Tr+1}(\rho) = (\mathbf{f}_r)_N(\rho) = \rho - \sum_{l=0}^{T-1} (\mathbf{f}_r)_{lr+1}(\rho).$$

□

The result above prove that equilibria are uniquely determined by the initial density ρ_0, which is constant in the spatially homogeneous case. More precisely, they do not depend on the number of grid points N and for any $\rho_0 \in [0, \rho_{\max}]$ the number of non zero distribution functions is determined by the acceleration term $\Delta v = V_{\max}/T$.

Remark 6 (Critical density). For $P \geq \frac{1}{2}$ (that is $\rho \leq \frac{1}{2}$ when taking $P = 1 - \rho$), the equilibrium distribution is $\mathbf{f}_r = [0, \dots, 0, \rho]$ and thus all vehicles travel at maximum speed. Only when $P < \frac{1}{2}$ the lower speed classes begin to fill up. The value of ρ for which $P = \frac{1}{2}$ is called *critical density*, and it influences the qualitative behaviour of macroscopic quantities. In particular, it determines the phase transition observed in fundamental diagrams, see §5 below.

Remark 7 (Unstable equilibria). Theorem 5 gives the uniqueness of the stable equilibria of the model. Unstable ones may occour if the initial condition is such that $f_1(0) = 0$. In fact, the interaction rules related to Ω_2 do not allow a post-interaction velocity v which is less than v^*. Thus if $f_1(0) = 0$, i.e. there are no vehicles with velocity $v_1 = 0$ at the initial time, there will not be interactions leading to an increase of f_1. This consideration can be generalized: if $f_j(0) = 0$ for $j = 1, \dots, \bar{j} < r$, then the computed equilibria will be $f_j = (\mathbf{f}_r)_{j-\bar{j}}$, where $\mathbf{f}_r$ is the stable equilibrium of Theorem 5. In this sense, the equilibrium solution of the δ model depends not only on ρ, but also on the initial condition $f(0)$. These solutions however are unstable: a small perturbation on $f_1(0)$ is enough to trigger the evolution towards the stable equilibrium, which depends only on ρ.

This is illustrated in Figure 4: in the left panel we show the evolution towards equlibrium when $f_j(0) \neq 0$ for all classes, while in the middle we show the case when $f_1 = f_2 = f_3 = 0$. In the rightmost panel we show a perturbation of the previous case, where f_1 takes a very small but nonzero value. It is clear that the evolution goes at first towards the unstable equilibrium of the middle panel, but then, at length, the stable equilibrium of Theorem 5 emerges.

4 The χ velocity model

A very reasonable doubt arises from the structure of the stable equilibria of the δ model. In fact one could argue that the equilibria depend on the particular choice of the acceleration interaction made in the δ model, in which a vehicle accelerates by jumping from its pre-interaction velocity v_* to the new velocity $v_* + \Delta v$. Thus it could seem quite natural that only velocities 0, Δv, $2\Delta v, \ldots, V_{\max}$ give a non zero contribution at equilibrium.

Here we study the χ model, already introduced in Section 2.1, in which vehicles can assume a post-interaction velocity uniformly distributed over a range of speeds when the acceleration interaction occurs. We will show that although this model is more refined than the δ model, at equilibrium the essential information is already caught by the simpler δ model.

Using the formulation (6) for the transition probability density A, we rewrite (2) as

$$\partial_t f = G_1[f,f](t,v) + G_2[f,f](t,v) - \eta f \int_V f^* dv^*,$$

where, defining Ω_1 and Ω_2 as in (3),

$$G_1[f,f](t,v) = \eta \int_{\Omega_1} \left[(1-P)\delta_{v_*}(v) + P \frac{\chi_{[v_*, \min\{v_*+\Delta v, V_{\max}\}]}(v)}{\min\{v_* + \Delta v, V_{\max}\} - v_*} \right] f_* f^* dv_* dv^*, \tag{17}$$

$$G_2[f,f](t,v) = \eta \int_{\Omega_2} \left[(1-P)\delta_{v^*}(v) + P\delta_{v_*}(v) \right] f_* f^* dv_* dv^*. \tag{18}$$

In G_1, the χ function can be split as

$$\frac{\chi_{[v_*, \min\{v_*+\Delta v, V_{\max}\}]}(v)}{\min\{v_* + \Delta v, V_{\max}\} - v_*} = \begin{cases} \frac{\chi_{[v_*, v_*+\Delta v]}(v)}{\Delta v}, & \text{if } v_* \in [0, V_{\max} - \Delta v] \\ \frac{\chi_{[v_*, V_{\max}]}(v)}{V_{\max} - v_*}, & \text{if } v_* \in [V_{\max} - \Delta v, V_{\max}] \end{cases}$$

and substituting in (17) and evaluating explicitly (18), we find:

$$\begin{aligned} G_1[f,f](t,v) =& \eta(1-P) f(t,v) \int_v^{V_{\max}} f^* dv^* + \eta \frac{P}{\Delta v} \int_0^{V_{\max}-\Delta v} f_* \chi_{[v_*, v_*+\Delta v]}(v) dv_* \int_{v_*}^{V_{\max}} f^* dv^* \\ &+ \eta P \int_{V_{\max}-\Delta v}^{V_{\max}} f_* \frac{\chi_{[v_*, V_{\max}]}(v)}{V_{\max} - v_*} dv_* \int_{v_*}^{V_{\max}} f^* dv^* \end{aligned} \tag{19}$$

$$G_2[f,f](t,v) = \eta(1-P) f(t,v) \int_v^{V_{\max}} f_* dv_* + \eta P f(t,v) \int_0^v f^* dv^*.$$

4.1 Discretization of the model

To compute the asymptotic kinetic distribution function of the χ model, we need to integrate the equations numerically. Thus we use the same discretization of the velocity space $[0, V_{\max}]$ introduced to discretize the δ model, see (9).

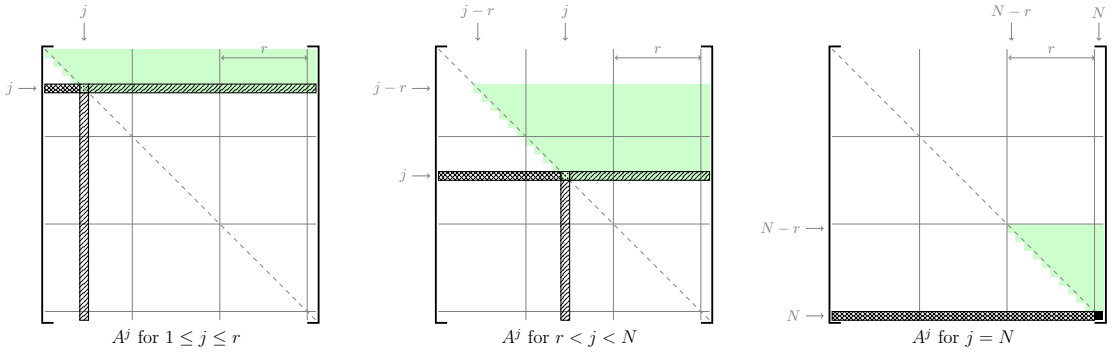

Figure 5: Structure of the interaction matrices resulting from the χ model.

Integrating the model (4) over each cell, we find the system of ODEs (10), but now the gain term is given by (19). Although in this case the integrals are laborious, they can be computed recalling that $\Delta v = V_{\max}/T$ with $T \in \mathbb{N}$ and assuming that Δv is a multiple of δv. Thus we will take $N - 1 \equiv 0 (\mathtt{mod}\, T)$ and $r = \frac{N-1}{T}$.

The details are reported in Appendix A and here we just point out that, as in the case of the δ model, the ODE system can be conveniently rewritten in vector form as

$$\frac{d}{dt} f_j = \eta \left[\mathbf{f}^{\mathsf{T}} A_\chi^j \mathbf{f} - \mathbf{f}^{\mathsf{T}} \mathbf{e}_j \mathbf{1}_N^{\mathsf{T}} \mathbf{f} \right], \quad j = 1, \dots, N \tag{20}$$

where $\mathbf{f} = [f_1, \dots, f_N]^{\mathsf{T}} \in \mathbb{R}^N$ is the vector of the unknown functions, $\mathbf{e}_j \in \mathbb{R}^N$ denotes the vector with a 1 in the j-th coordinate and 0's elsewhere, $\mathbf{1}_N^{\mathsf{T}} = [1, \dots, 1] \in \mathbb{R}^N$ and A_χ^j is the j-th interaction matrix such that $\left(A_\chi^j\right)_{hk}$ contains the probabilities that a candidate vehicle with velocity in I_h interacting with a field vehicle with velocity in I_k will acquire a velocity in I_j.

Since the matrices appearing in (20) are again stochastic, we can apply Theorem 4 to guarantee existence and well posedness of the solution.

In Figure 5 we show the structure of the χ matrices: they are less sparse than the δ matrices because of the uniformly distributed acceleration in $[v_*, v_* + \Delta v]$, where v_* is the pre-interaction speed. In fact the matrix A_χ^j contains non zero elements also on the rows from the $(j - r + 1)$-th to the $(j - 1)$-th, see the shaded areas in Figure 5, which represent non zero probabilities of accelerating to a speed in I_j and, since $\Delta v = r\delta v$, exactly r rows fill up. Instead, the area drawn using hatching contains the same probabilities already shown in Figure 1 for the case of the δ model. Thus, in contrast to the δ model, steady solutions of the ODE system (20) depend on the number of velocities N chosen to discretize the χ model.

Moreover, all the elements on the rows $j - r, \dots, j - 1$ of the matrix A_χ^j, $j = 1, \dots, N$, tend to 0 as $1/r$ when the grid is refined. In particular, for $j = 1, \dots, r$, $A_\chi^j \to A_\delta^j$. The previous consideration is not true for the matrices A_χ^j, for $j = r + 1, \dots, N$.

Despite their differences the χ and the δ model are deeply related. This can be seen computing the expected output speed in each model resulting from a fixed pre-interaction speed. We define the expected value $< v >$ of the post-interaction velocity as

$$< v >= \int_0^{V_{\max}} v A(v_* \to v | v^*, \rho)\, dv, \quad (v_*, v^*) \in [0, V_{\max}]^2 . \tag{21}$$

For brevity we indicate with $A_\delta(v)$ and $A_\chi(v)$ the probability density given in (5) and (6) respectively. Since both $A_\delta(v)$ and $A_\chi(v)$ depend on the position of the pair (v_*, v^*) in $[0, V_{\max}]^2$,

then (21) can be split:

$$< v >= \begin{cases} \displaystyle\int_0^{V_{\max}} v A_1(v)\, dv, & \text{if } (v_*, v^*) \in \Omega_1 \\ \displaystyle\int_0^{V_{\max}} v A_2(v)\, dv, & \text{if } (v_*, v^*) \in \Omega_2 \end{cases} \tag{22}$$

Since $A_\delta(v)$ and $A_\chi(v)$ differ only in the subset Ω_1, the expected speed resulting from the second equation of (22) is the same both for δ and χ models and it does not depend on the acceleration parameter Δv. For this reason we compute $< v >$ only in Ω_1. In the case of the δ model we obtain:

$$\begin{aligned} < v >_\delta &= \int_0^{V_{\max}} v \left[(1-P)\, \delta_{v_*}(v) + P\, \delta_{\min\{v_*+\Delta v, V_{\max}\}}(v) \right] dv \\ &= (1-P)\; v_* + P \begin{cases} v_* + \Delta v_\delta, & \text{if } v_* + \Delta v_\delta < V_{\max} \\ v_* + (V_{\max} - v_*)\,, & \text{if } v_* + \Delta v_\delta > V_{\max} \end{cases} \end{aligned} \tag{23}$$

In contrast, if we consider the χ model we have

$$\begin{aligned} &\int_0^{V_{\max}} v \left[(1-P)\, \delta_{v_*}(v) + P\, \frac{\chi_{[v_*, \min\{v_*+\Delta v, V_{\max}\}]}(v)}{\min\{v_* + \Delta v, V_{\max}\} - v_*} \right] dv \\ &\qquad = (1-P)\; v_* + P \begin{cases} \dfrac{1}{\Delta v} \displaystyle\int_{v_*}^{v_*+\Delta v} v\, dv, & \text{if } v_* + \Delta v < V_{\max} \\ \dfrac{1}{V_{\max} - v_*} \displaystyle\int_{v_*}^{V_{\max}} v\, dv, & \text{if } v_* + \Delta v > V_{\max} \end{cases} \end{aligned}$$

and thus

$$< v >_\chi = (1-P)\; v_* + P \begin{cases} v_* + \dfrac{\Delta v_\chi}{2}, & \text{if } v_* + \Delta v_\chi < V_{\max} \\ v_* + \dfrac{1}{2}\,(V_{\max} - v_*), & \text{if } v_* + \Delta v_\chi > V_{\max} \end{cases} \tag{24}$$

By comparing the last lines of (23) and (24), it is clear that

$$< v >_\chi = < v >_\delta \qquad \forall\, v_* < V_{\max} - \Delta v_\chi, \qquad \text{provided } \Delta v_\delta = \tfrac{1}{2} \Delta v_\chi. \tag{25}$$

Remark 8. Let's compare the A_χ^j matrices (Figure 5) for $r < j < N$ with a given Δv and the corresponding A_δ^j matrices (Figure 1) with $\frac{\Delta v}{2}$. The isolated nonzero row of A_δ^j is at $j - \frac{r}{2}$, which corresponds to the middle of the green shaded area in A_χ^j. Morevover, for any fixed Δv, it can be proven that the sum of the quantities located in the shaded area of A_χ is equal to the total contribution provided by the $\left(j - \frac{r}{2}\right)$-th row of the δ matrices obtained with the acceleration parameter $\frac{\Delta v}{2}$. In other words the total effect of the $\left(j - \frac{r}{2}\right)$-th row of A_δ^j with $\frac{\Delta v}{2}$ is spread over $r+1$ rows in the matrices A_χ^j with Δv, which are the rows shaded in green in Figure 5.

5 Macroscopic properties

In order to explain the relation of Δv with the acceleration of the vehicles in the model, we compute

$$\begin{aligned}\frac{\partial u}{\partial t} &= \frac{\partial}{\partial t}\left[\frac{1}{\rho}\int_V v f(t,v)\,dv\right] = \frac{1}{\rho}\int_V v Q[f,f](t,v)\,dv \\ &= \frac{\eta}{\rho}\left[\int_V v\,dv\int_V\int_V A(v_*\to v|v^*;\rho) f_* f^*\,dv_* dv^* - \rho\int_V v f(t,v)\,dv\right] \\ &= \frac{\eta}{\rho}\left[\int_V\int_V < v > f_* f^*\,dv_* dv^* - \rho\int_V v f(t,v)\,dv\right]\end{aligned}$$

where $< v >= \int_V v A(v_*\to v|v^*;\rho)\,dv$ is a function of v_* and v^*.

In the case of the δ model, $< v >_\delta$ is given by (23) for $(v_*, v^*) \in \Omega_1$, while $< v >_\delta = (1-P)v^* + Pv_*$ for $(v_*, v^*) \in \Omega_2$ and thus

$$\begin{aligned}\frac{\partial u}{\partial t} = \frac{\eta}{\rho}\Bigg[&(1-P)\int_0^{V_{\max}}\int_0^{v_*} v^* f_* f^*\,dv^* dv_* + P\int_0^{V_{\max}}\int_0^{v_*} v_* f_* f^*\,dv^* dv_* + \\ &(1-P)\int_0^{V_{\max}}\int_{v_*}^{V_{\max}} v_* f_* f^*\,dv^* dv_* + P\int_0^{V_{\max}-\Delta v}\int_{v_*}^{V_{\max}} (v_*+\Delta v) f_* f^*\,dv^* dv_* + \\ &P\int_{V_{\max}-\Delta v}^{V_{\max}}\int_{v_*}^{V_{\max}} V_{\max} f_* f^*\,dv^* dv_* - \rho\int_0^{V_{\max}} v f(t,v)\,dv\Bigg].\end{aligned}$$

Given an initial distribution $f(t=0,v)$, the equation above yields the evolution of the macroscopic acceleration in time. It is easy to study analytically this quantity at the initial time. In particular, we compute the initial acceleration for the case in which all vehicles are steady, but the density is below the critical value (defined in Remark 6). By considering an initial distribution with all vehicles in the lowest velocity class, i.e. of the form $f(0,v) = \frac{2\rho}{\delta v}\chi_{I_1}(v)$, we have

$$\left.\frac{\partial u}{\partial t}\right|_{t=0} = \frac{\eta}{\rho} P\Delta v_\delta \int_0^{V_{\max}-\Delta v}\int_{v_*}^{V_{\max}} f_* f^*\,dv^* dv_* + \mathcal{O}(\delta v) = \frac{1}{2}\rho\eta P\Delta v_\delta + \mathcal{O}(\delta v)$$

The above equation shows that the acceleration of the vehicles in the δ model depends linearly on Δv. Analogously, for the χ model, using (24), one obtains

$$\left.\frac{\partial u}{\partial t}\right|_{t=0} = \frac{1}{4}\rho\eta P\Delta v_\chi + \mathcal{O}(\delta v)$$

which reinforces the remark made in (25) about the similarities of the χ and the δ model when $\Delta v_\chi = 2\Delta v_\delta$.

Remark 9 (Acceleration). Recall that $(\eta\rho)^{-1}$ have dimension of time. Thus $\eta\rho\Delta v$ is the built-in acceleration of the model, which, not surprisingly, is linked to Δv. We can use dimensional arguments to estimate the order of magnitude of Δv. According to Lebacque [13], the maximum acceleration of cars is approximately $a_{LB} = 2.5$ m/sec^2. The maximum speed is approximately $\mathbb{V}_M \simeq 28$m/sec, and we expect the maximum acceleration when $P = 1$. Thus $\frac{1}{2}\eta\rho\Delta v \simeq a_{LB}/\mathbb{V}_M$. For a typical value $\eta\rho = 1$, this gives $T \simeq \frac{1}{2}\mathbb{V}_M/a_{LB} \simeq 6$.

This argument indicates that the model is expected to provide reliable results for relatively small values of T.

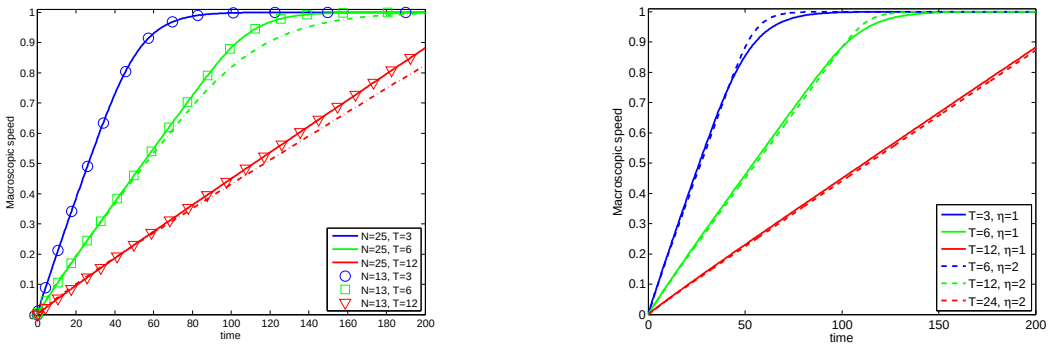

Figure 6: Evolution of the macroscopic velocity in time. Left: comparison of different values of Δv and δv. Right: relaxation to steady state for different combinations of η and T. The dashed lines correspond to the χ model.

The estimates above provide the behaviour of the macroscopic acceleration at the initial time. We now study the evolution of the macroscopic velocity u in time, up to steady state. These data are shown in Fig. 6 and Fig. 7, for various combinations of the model parameters. The results shown are obtained integrating the equations for the δ and the χ model found in (12) and (20), respectively, and computing at each time $u(t) = \frac{1}{\rho}\int_V v f(t,v)\, dv$.

Figure 6 shows a typical case in which we expect *acceleration*. The density is $\rho = 0.15$, well below the critical value, and we start with an initial distribution in which $f_1(t=0) = \rho$, while $f_j(t=0) = 0, j \geq 2$. Thus initially all vehicles are still, and, since the density is low, they will accelerate to reach the maximum speed. The duration of the transient depends on the product $\eta\Delta v = \eta/T$, for a fixed density, as is apparent in the right panel of the figure, because the acceleration, i.e. the slope of the curves, is proportional to $\eta\Delta v$. The left panel shows the effect of the grid discretization, i.e. the role of $\delta v = 1/(N-1)$. It is clear that the discretization grid has no influence on the results, as expected from Theorem 5. The dashed lines show the evolution of the macroscopic velocity obtained with the χ model. The colour code is chosen to ensure that the curves with $\Delta v_\delta = \frac{1}{2}\Delta v_\chi$ are drawn in the same colour. As expected, the macroscopic velocity for the χ and the δ model behave very similarly, provided the parameter Δv is chosen correctly.

Next, in Figure 7, we show the evolution of the macroscopic velocity in two cases when we expect *deceleration*. Namely, we consider $\rho = 0.65$ in the left panel, while $\rho = 0.9$ in the right panel. The initial distribution is $f_N(t=0) = \rho - \epsilon$, $f_1(t=0) = \epsilon$, and $f_j(t=0) = 0, j = 2, \ldots, N-1$. The value ϵ is introduced to ensure convergence to the stable equilibrium, see Remark 7. Here $\epsilon = 0.01$. In other words, we start with a congested traffic, in which initially almost all cars are driving at the fastest speed available. Clearly, this situation is somewhat artificial, but surely we expect the cars to brake. Since braking does not depend on Δv, we expect that the relaxation time towards equilibrium depends mainly on η and only weakly on T. This is clearly seen in both pictures. The macroscopic speed to which the model relaxes on the other hand will depend on Δv and on ρ, but not on η. Note that when $\rho = 0.9$, in all cases considered here, the equilibrium speed is zero: in fact the traffic is extremely jammed. For $\rho = 0.65$ instead, we expect that the traffic will have a residual speed, because we are well above the critical density, but cars are not "bumper to bumper", and this residual speed does depend on Δv.

As already discussed in the previous section, the non zero elements of the matrix A_χ can be

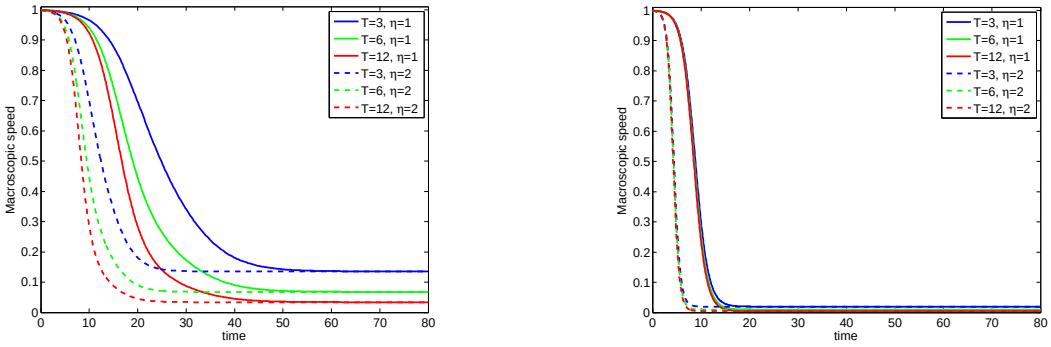

Figure 7: Evolution of the macroscopic velocity in time, for different values of T and η. Left: $\rho = 0.65$. Right: $\rho = 0.9$

lumped in the matrix A_δ for N sufficiently large, with the only exception of the elements in the bottom right corner $r \times r$ of the matrix. This is shown, for instance, in the evaluation of the expected value of the resulting speeds due to acceleration interactions in (23) and (24), which are comparable, except again for the high speed values. Thus, although the χ model is apparently more refined then the δ model, we expect that both models will provide similar macroscopic information, for N large. This is usually analyzed by computing the density and the flux as moments of the asymptotic kinetic distribution $f^\infty(v)$

$$\rho = \int_0^{V_{\max}} f^\infty(v)\, dv, \quad (\rho u) = \int_0^{V_{\max}} v f^\infty(v)\, dv \tag{26}$$

and by studying the characteristics of the related *fundamental diagram* which is obtained plotting the flux against the density. Moreover, Theorem 5 ensures that for the δ model, only few velocities, those obtained with $\Delta v = \delta v$, are necessary to describe completely the asymptotic kinetic distribution. We expect therefore that the macroscopic behaviour of the δ model will be apparent even on very coarse velocity grids, i.e. for $r = 1$.

In Figure 8 we show the fundamental diagrams provided by the δ model (blue curves) and the χ model (red curve), computed with $\Delta v_\delta = \frac{1}{2}\Delta v_\chi$, for two different values of Δv_δ. In the left panel, $r = 1$, while $r = 20$ on the right. The figure shows that the diagram of the χ model is very similar to the diagram of the δ model when $N \to \infty$ and this result is in agreement with the fact that the expected output speed of the two models is the same when choosing the acceleration parameter of the δ model as a half of the acceleration parameter of the χ model. The only difference is provided by the maximum speeds which, as already noted, are slightly different. Note that the similarity of the fundamental diagrams does not mean that the asymptotic equilibrium functions of the χ and of the δ model converge to the same function as N approaches ∞.

Observe that the fundamental diagrams given by the δ model in both plots in each line of Figure 8 use the same information. In fact, following the results of Theorem 5, the macroscopic flux is given by

$$\text{Flux}_\delta(r) = \int_0^{V_{\max}} v f^\infty(v) dv = \sum_{j=1}^{N} (\mathbf{f}_r)_j \frac{1}{|I_j|} \int_{I_j} v\, dv = \sum_{l=1}^{T+1} (\mathbf{f}_1)_l v_{(l-1)r+1}$$

where v_j denotes the center of the cell I_j. Recalling the definition of I_j, we have that $v_1 = \Delta v/4r$,

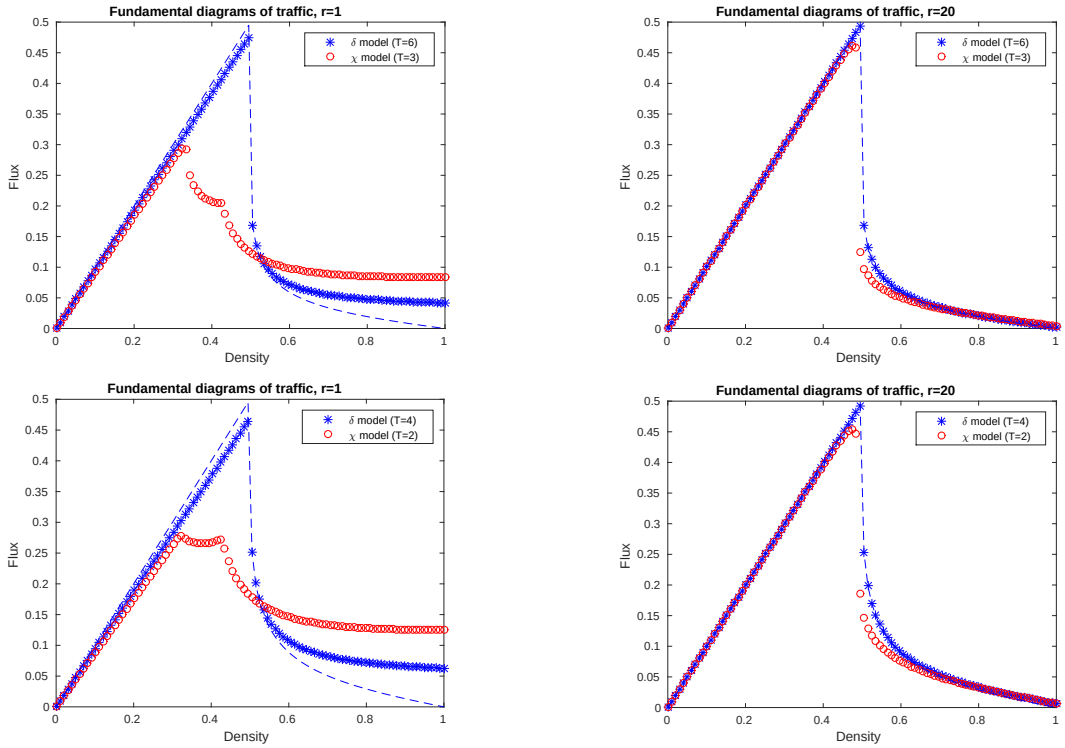

Figure 8: Fundamental diagrams resulting from the δ model (blue *-symbols) and from the χ model with acceleration parameter $\Delta v_\delta = \frac{1}{2}\Delta v_\chi$ (red circles). The dashed line is the flux of the δ model in the limit $r \to \infty$.

$v_N = V_{\max} - \Delta v/4r$ and $v_{(l-1)r+1} = (l-1)\Delta v$. Thus, in order to compute the fundamental diagram of the δ model with any value of r, it is enough to compute the equilibrium distribution $\mathbf{f}_1$ using $r = 1$ and then compute the flux with the formula above. In particular, using only $\mathbf{f}_1$, one may also compute the fundamental diagram of the δ model also in the limit $r \to \infty$ with the formula

$$\mathrm{Flux}_\delta(\infty) = \sum_{l=1}^{T+1} (\mathbf{f}_1)_l (l-1)\Delta v.$$

The dashed blue line in all panels of Figure 8 shows the quantity $\mathrm{Flux}_\delta(\infty)$ just defined. Note that in the case of the χ model, for each value of r, one has to compute the full equilibrium distribution with $N = rT + 1$ velocities.

When increasing r, we observe that the flux at $\rho_{\max}$ approaches zero. This is because for $\rho = \rho_{\max}$, $(\mathbf{f}_1)_1$ is the only non zero component at equilibrium, all vehicles travel at a velocity in the lowest speed class I_1 and the flux is therefore $\frac{\Delta v}{4r}(\mathbf{f}_1)_1$. Similarly, in the free phase, i.e. below the critical density, all vehicles travel at a velocity in the highest speed class I_N and the flux is therefore $(V_{\max} - \frac{\Delta v}{4r})(\mathbf{f}_1)_{T+1} = (V_{\max} - \frac{\Delta v}{4r})\rho$. The free-phase flux is therefore linear in ρ and its slope approaches $V_{\max}$ when $r \to \infty$.

In Figure 8, we observe that both models provide a sharp decrease in the flux, beyond the critical density. This phenomenon is well known in traffic modelling, and it is called *capacity drop*, see [23] and references therein. The critical density marks the transition from free to congested

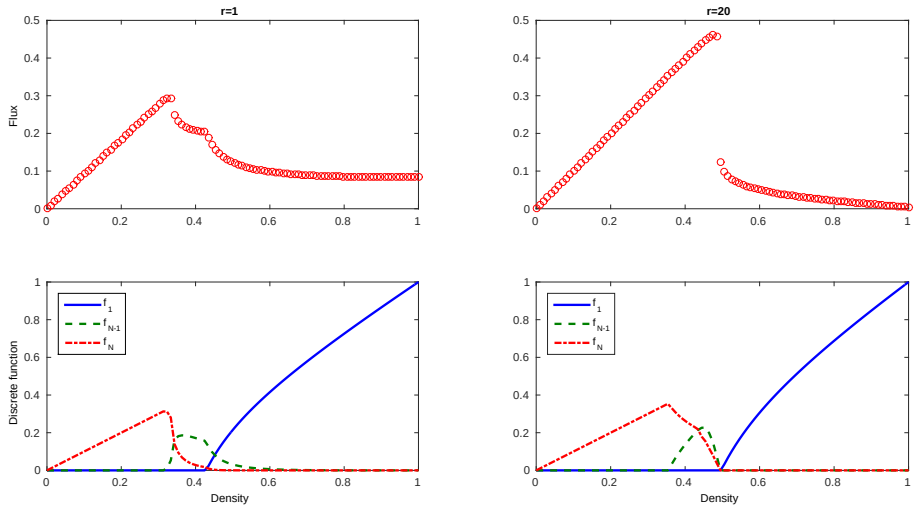

Figure 9: Top: fundamental diagrams provided by the χ model with $N = 4$ (left) and $N = 61$ (right) velocities. Bottom: equilibria of the function f_1 (blue solid line), f_{N-1} (green dashed) and f_N (red dot-dashed) for any density in $[0, 1]$.

flow and it corresponds to a bifurcation of the equilibrium solutions computed in Theorem 5 for the case of the δ model. Thus, the physical concept of phase transition in traffic flow theory has a rigorous mathematical counterpart in the present models.

Remark 10. Observe that the critical density of the χ model approaches the critical density of the δ model when $N \to \infty$. In fact, since the matrix $A^1_\chi \to A^1_\delta$ for $r \to \infty$, we also have that $(\mathbf{f}^\chi_r)_1 \to \left(\mathbf{f}^\delta_1\right)_1$. More precisely, the analogous of (14) for the χ model is

$$\left(\frac{3P-2}{2} - \frac{P}{12r}\right) f_1^2 + \left(1 - 2P + \frac{P}{4r}\right) \rho f_1 = 0$$

and the stable equilibrium is thus

$$\begin{cases} 0 & P \geq \frac{4r}{8r-1} \\ 2\frac{2P-1}{3P-2}\rho + \mathcal{O}(\frac{1}{r}) & \text{otherwise} \end{cases}$$

In Figure 9 we show the fundamental diagrams of the χ model for $r = 1$ and $r = 20$, together with a few representative f_j's at equilibrium, as functions of ρ. In the left part, for $r = 1$, two phase transitions appear in the fundamental diagram (top left). Comparing with the bottom left plot, the origin of this phenomenon can be appreciated. A first transition occurs when the density becomes large enough to oblige a few drivers to brake: thus the second largest speed class I_{N-1} starts being populated (green dashed curve), while the fastest speed class begins to be depleted (red curve). A second transition occurs when some vehicles enter the lowest speed class (blue curve). This latter transition is the one that, when increasing r, moves towards the critical density $\rho = 1/2$, see Remark 10. The first phase transition is not observable for large r, because f^∞_{N-1} is related to the velocity $v_{N-1} \to V_{\max}$, as $\delta v \to 0$, so that the transition of vehicles from I_N to I_{N-1} is not enough to determine an abrupt change in the flux.

6 Conclusions and perspectives

In this work we have introduced two kinetic models for vehicular traffic, in which we have assumed a continuous space of microscopic speeds. For the time being, we analyze the space homogeneous case, to study the asymptotic behaviour of the distribution function.

As in [7], we consider a Boltzmann-like term based on binary interactions. Our models are characterized by a parameter Δv, that has physical relevance and is related to the maximum speed variation in a unit of time. The models are defined by the probability density of gaining or losing a given velocity and they differ only in the modeling of acceleration interaction.

First of all we have studied the case in which the resulting speed after an acceleration is obtained by a velocity jump from v_* to $v_* + \Delta v$, where v_* is the pre-interaction speed. We have referred to this model as δ model and we have proved that its asymptotic kinetic function is an atomic distribution with respect to the velocity variable; in other words it is a combination of Dirac delta functions centered at a finite number of velocities. The number T of delta functions contributing to the equilibrium distribution is controlled by the acceleration parameter through the relation $\Delta v = V_{\max}/T$, irrespective of the numerical discretization of velocity space. This result means that, under suitable and reasonable assumptions on the microscopic interactions, the number of discrete velocities necessary to completely describe the equilibrium distribution function is implicitly determined by the acceleration parameter Δv. One of the consequences of this result is that the discrete velocity approach of [7] is made robust because the distance of two adjacent velocities in the discrete lattice, can now be given a physical meaning. On the other hand, our kinetic model is computationally efficient because it can describe macroscopic phenomena using only $V_{\max}/\Delta v$ velocities, without the need for a finer discretization in velocity space.

Instead, in the χ model we have prescribed the acceleration interaction in a way that is closer to the modeling given by Klar and Wegener in [10], but again respecting the physical relevance of Δv. In fact, we have assumed that the output speed after an acceleration is uniformly distributed over the range $[v_*,\, v_* + \Delta v]$. We show that the χ model with acceleration parameter Δv gives a similar macroscopic behaviour of traffic provided by the simpler δ model with acceleration parameter $\Delta v/2$, as we see comparing the fundamental diagrams of both models, notwithstanding the fact that the asymptotic distribution function does not converge to that of the δ model. Thus the χ model, despite the more realistic description of interactions, at least at equilibrium, gives the same information of the simpler and computationally much cheaper δ model.

We study the evolution in time of the macroscopic velocity, and its relation with the parameter Δv, showing how this parameter determines the macroscopic acceleration.

The results obtained in this work suggest that a small number of velocities is suitable for the kinetic modeling of traffic. This is crucial to make kinetic modeling of complex traffic flows amenable to computations. A natural development is to extend the results obtained here to the spatially inhomogeneous case. We expect that our approach might permit the discretization of the full kinetic equation using a very small number of microscopic velocities, with a lattice chosen on the basis of the parameter Δv endowed with physical meaning. We also plan to extend our study to the case of multipopulation kinetic models, as we proposed in [21].

Moreover, since the equilibrium solutions of the δ model can be explicitly computed, the results of this work provide a natural closure law for a possible macroscopic model.

References

[1] A. Aw, A. Klar, T. Materne, and M. Rascle. Derivation of continuum traffic flow models from microscopic follow-the-leader models. *SIAM J. Appl. Math.*, 63(1):259–278, 2002.

[2] A. Aw and M. Rascle. Resurrection of "second order" models of traffic flow. *SIAM J. Appl. Math.*, 60(3):916–938 (electronic), 2000.

[3] R. Borsche, M. Kimathi, and A. Klar. A class of multi-phase traffic theories for microscopic, kinetic and continuum traffic models. *Comput. Math. Appl.*, 64:2939–2953, 2012.

[4] V. Coscia, M. Delitala, and P. Frasca. On the mathematical theory of vehicular traffic flow. II. Discrete velocity kinetic models. *Internat. J. Non-Linear Mech.*, 42(3):411–421, 2007.

[5] M. Delitala and A. Tosin. Mathematical modeling of vehicular traffic: a discrete kinetic theory approach. *Math. Models Methods Appl. Sci.*, 17(6):901–932, 2007.

[6] L. Fermo and A. Tosin. A fully-discrete-state kinetic theory approach to modeling vehicular traffic. *SIAM J. Appl. Math.*, 73(4):1533–1556, 2013.

[7] L. Fermo and A. Tosin. Fundamental diagrams for kinetic equations of traffic flow. *Discrete Contin. Dyn. Syst. Ser. S*, 7(3):449–462, 2014.

[8] M. Herty and R. Illner. On stop-and-go waves in dense traffic. *Kinet. Relat. Models*, 1(3):437–452, 2008.

[9] M. Herty and R. Illner. Analytical and numerical investigations of refined macroscopic traffic flow models. *Kinet. Relat. Models*, 3(2):311–333, 2010.

[10] A. Klar and R. Wegener. A kinetic model for vehicular traffic derived from a stochastic microscopic model. *Transport Theory Statist. Phys.*, 25:785–798, 1996.

[11] A. Klar and R. Wegener. Enskog-like kinetic models for vehicular traffic. *J. Stat. Phys.*, 87:91, 1997.

[12] A. Klar and R. Wegener. Traffic flow: models and numerics. In *Modeling and computational methods for kinetic equations*, Model. Simul. Sci. Eng. Technol., pages 219–258. Birkhäuser Boston, Boston, MA, 2004.

[13] J. P. Lebacque. Two-phase bounded-acceleration traffic flow model: analytical solutions and applications. *Transportation Research Record*, 1852:220–230, 2003.

[14] J. P. Lebacque and M. M. Khoshyaran. A variational formulation for higher order macroscopic traffic flow models of the gsom family. *Procedia - Social and Behavioral Sciences*, 80:370–394, 2013.

[15] M. J. Lighthill and G. B. Whitham. On kinematic waves. II. A theory of traffic flow on long crowded roads. *Proc. Roy. Soc. London. Ser. A.*, 229:317–345, 1955.

[16] A. R. Méndez and R. M. Velasco. Kerner's free-synchronized phase transition in a macroscopic traffic flow model with two classes of drivers. *J. Phys. A: Math. Theor.*, 46, 2013.

[17] S. L. Paveri-Fontana. On Boltzmann-like treatments for traffic flow: a critical review of the basic model and an alternative proposal for dilute traffic analysis. *Transportation Res.*, 9(4):225–235, 1975.

[18] B. Piccoli and A. Tosin. Vehicular traffic: A review of continuum mathematical models. In R. A. Meyers, editor, *Encyclopedia of Complexity and Systems Science*, volume 22, pages 9727–9749. Springer, New York, 2009.

[19] I. Prigogine. A Boltzmann-like approach to the statistical theory of traffic flow. In R. Herman, editor, *Theory of traffic flow*, pages 158–164, Amsterdam, 1961. Elsevier.

[20] I. Prigogine and R. Herman. *Kinetic theory of vehicular traffic*. American Elsevier Publishing Co., New York, 1971.

[21] G. Puppo, M. Semplice, A. Tosin, and G. Visconti. Fundamental diagrams in traffic flow: the case of heterogeneous kinetic models. *Commun. Math. Sci.*, 2015.

[22] M. Rosini. *Macroscopic models for vehicular flows and crowd dynamics: theory and applications*. Springer, Basel, Switzerland, 2013.

[23] H. M. Zhang and T. Kim. A car-following theory for multiphase vehicular traffic flow. *Transportation Research Part B: Methodological*, 39(5):385–399, 2005.

A Matrix elements for the discretization of the χ model

In order to compute the A^j_χ matrices, we observe that the gain operator of the δ model given in (8) differs from the gain operator of the χ model only in the last two terms of G_1 appearing in the equation (19). Therefore, we just show the terms resulting from:

$$\begin{aligned}\widetilde{G_1}[f,f](t,v) =& \frac{P}{\Delta v}\int_0^{V_{\max}-\Delta v} f_*\chi_{[v_*,v_*+\Delta v]}(v)dv_*\int_{v_*}^{V_{\max}} f^*dv^* \\ &+ P\int_{V_{\max}-\Delta v}^{V_{\max}} f_*\frac{\chi_{[v_*,V_{\max}]}(v)}{V_{\max}-v_*}dv_*\int_{v_*}^{V_{\max}} f^*dv^*dv.\end{aligned}$$

When the terms above are integrated over the cells V_1, we get

$$\int_{V_1}\widetilde{G_1}[f,f](t,v)dv = \frac{P}{6r}f^jf_j + \frac{P}{4r}f_j\sum_{k=j+1}^{N} f^k. \tag{27a}$$

For $j = 2,\dots,r$:

$$\int_{V_j}\widetilde{G_1}[f,f](t,v)dv = \frac{P}{r}\sum_{h=1}^{j-1} f_h\left[\frac{1}{2}f^h + \sum_{k=h+1}^{N} f^k\right] + \frac{P}{3r}f^jf_j + \frac{P}{2r}f_j\sum_{k=j+1}^{N} f^k \tag{27b}$$

For $j = r+1$,

$$\begin{aligned}\int_{V_{r+1}}\widetilde{G_1}[f,f](t,v)dv =& \frac{P}{3r}f^{j-r}f_{j-r} + \frac{3P}{4r}f_{j-r}\sum_{k=j-r+1}^{N} f^k \\ &+ \frac{P}{r}\sum_{h=j-r+1}^{j-1} f_h\left[\frac{1}{2}f^h + \sum_{k=h+1}^{N} f^k\right] + \frac{P}{3r}f^jf_j + \frac{P}{2r}f_j\sum_{k=j+1}^{N} f^k,\end{aligned} \tag{27c}$$

For $j = r+2,\dots,N-r-1$,

$$\begin{aligned}\int_{V_j}\widetilde{G_1}[f,f](t,v)dv =& \frac{P}{6r}f^{j-r}f_{j-r} + \frac{P}{2r}f_{j-r}\sum_{k=j-r+1}^{N} f^k \\ &+ \frac{P}{r}\sum_{h=j-r+1}^{j-1} f_h\left[\frac{1}{2}f^h + \sum_{k=h+1}^{N} f^k\right] + \frac{P}{3r}f^jf_j + \frac{P}{2r}f_j\sum_{k=j+1}^{N} f^k,\end{aligned} \tag{27d}$$

For $j = N - r$,

$$\begin{aligned}\int_{V_{N-r}} \widetilde{G_1}[f,f](t,v)dv =& \frac{P}{6r} f^{j-r} f_{j-r} + \frac{P}{2r} f_{j-r} \sum_{k=j-r+1}^{N} f^k \\ &+ \frac{P}{r} \sum_{h=j-r+1}^{j-1} f_h \left[\frac{1}{2} f^h + \sum_{k=h+1}^{N} f^k\right] \\ &+ P\left[\frac{7}{24r} + \frac{3}{8} - \frac{r}{2} + \left(\frac{1}{2} - r\right)^2 \log\left(\frac{2r}{2r-1}\right)\right] f^j f_j \\ &+ P\left[\frac{3}{8r} + \frac{1}{2} + \left(\frac{1}{2} - r\right)^2 \log\left(\frac{2r}{2r-1}\right)\right] f_j \sum_{k=j+1}^{N} f^k\end{aligned} \tag{27e}$$

For $j = N - r + 1, \ldots, N - 1$,

$$\begin{aligned}\int_{V_j} \widetilde{G_1}[f,f](t,v)dv =& \frac{P}{6r} f^{j-r} f_{j-r} + \frac{P}{2r} f_{j-r} \sum_{k=j-r+1}^{N} f^k \\ &+ \frac{P}{r} \sum_{h=j-r+1}^{j-1} f_h \left[\frac{1}{2} f^h + \sum_{k=h+1}^{N} f^k\right] \\ &+ P\left[\frac{3+4r}{8r} + \left(\frac{1}{2} - r\right)^2 \log\left(\frac{2r}{2r-1}\right)\right] f^{N-r} f_{N-r} \\ &+ P\left[\frac{1}{2r} + \log\left(\frac{2r}{2r-1}\right)\right] f_{N-r} \sum_{k=N-r+1}^{N} f^k \\ &+ P \sum_{h=N-r+1}^{j-1} \left[1 + \left(h + \frac{1}{2} - N\right) \log\left(\frac{N-h+\frac{1}{2}}{N-h-\frac{1}{2}}\right)\right] f^h f_h \\ &+ P \sum_{h=N-r+1}^{j-1} \log\left(\frac{N-h+\frac{1}{2}}{N-h-\frac{1}{2}}\right) f_h \sum_{k=h+1}^{N} f^k, \\ &+ P\left[j + 1 - N + \left(j + \frac{1}{2} - N\right)^2 \log\left(\frac{N-j+\frac{1}{2}}{N-j-\frac{1}{2}}\right)\right] f^j f_j \\ &+ P\left[1 + \left(j + \frac{1}{2} - N\right) \log\left(\frac{N-j+\frac{1}{2}}{N-j-\frac{1}{2}}\right)\right] f_j \sum_{k=j+1}^{N} f^k\end{aligned} \tag{27f}$$

Finally, for $j = N$,

$$\int_{V_N} \widetilde{G_1}[f,f](t,v)dv = P\left[\frac{1+3r}{12r} + \frac{1}{2}\left(\frac{1}{2}-r\right)\log\left(\frac{2r}{2r-1}\right)\right] f^{j-r} f_{j-r} \tag{27g}$$
$$+ P\left[\frac{1}{8r} + \frac{1}{2}\log\left(\frac{2r}{2r-1}\right)\right] f_{j-r} \sum_{k=N-r+1}^{N} f^k$$
$$+ P\sum_{h=j-r+1}^{j-1}\left[\frac{1}{2} + \frac{1}{2}\left(h+\frac{1}{2}-N\right)\log\left(\frac{N-h+\frac{1}{2}}{N-h-\frac{1}{2}}\right)\right] f^h f_h$$
$$+ P\sum_{h=j-r+1}^{j-1}\frac{1}{2}\log\left(\frac{N-h+\frac{1}{2}}{N-h-\frac{1}{2}}\right) f_h \sum_{k=h+1}^{N} f^k + \frac{P}{2} f^j f_j$$

In the formulae above, the distribution of the field and of the candidate vehicles are distinguished by the position of the index of the components of $\mathbf{f}$: bottom right for the candidate vehicles (as f_h), top right for the field vehicles (f^k). The matrices A^j_χ can be formed by removing the underlined terms in (11) and adding the contributions given in (27).